

Optical circular dichroism of single-wall carbon nanotubes

Ariadna Sanchez-Castillo,¹ C. E. Román-Velázquez,²

Cecilia Noguez,² and L. Meza-Montes¹

¹Instituto de Física, Universidad Autónoma de Puebla,

Apartado Postal J-48, Puebla 72570, México

²Instituto de Física, Universidad Nacional Autónoma de México,

Apartado Postal 20-364, D.F. 01000, México

(Dated: April 14, 2024)

Abstract

The circular dichroism (CD) spectra of single-wall carbon nanotubes are calculated using a dipole approximation. The calculated CD spectra show features that allow us to distinguish between nanotubes with different angles of chirality, and diameters. These results provide theoretical support for the quantification of chirality and its measurement, using the CD lineshapes of chiral nanotubes. It is expected that this information would be useful to motivate further experimental studies.

PACS numbers: 78.67.Ch, 81.07.De, 78.20.Bh, 78.40.Ri

I. INTRODUCTION

A century ago Lord Kelvin stated, "I call any geometrical figure, or group of points, chiral, and say that it has chirality, if its image in a plane mirror, ideally realized, cannot be brought to coincide with itself." According to Kelvin's definition, one could say only whether an object is chiral or not (achiral), and inferring that chirality is a purely geometrical property there is not reason to relate it to chemistry, physics or biology. Decades before, Louis Pasteur discovered a connection between optical activity and molecular chirality, and found that substances with the same elementary composition have different physical properties that led him to suppose that forces of nature are not mirror-symmetric. Today, we know that chirality plays an important role in chemistry, physics and biology and that left-amino acids and left-peptides are predominant in the living world.^{1,2} Despite of the simplicity of Kelvin's definition of chirality, there is not an algorithm for such a criterion to diagnostic chirality.^{3,4,5} There are several works which have attempted to estimate chirality quantitatively, however, they have not succeeded to find an universal approach which gives unambiguous results.^{6,7,8,9,10,11,12,13,14} Furthermore, a drawback of these attempts to quantify chirality is that they do not provide a way to compare directly with experimental observations.

Among nanostructures, carbon nanotubes are known to be chiral. The atomic structure of single-wall carbon nanotubes (SWNTs) resembles the wrapping of a sheet of carbons located in a two-dimensional hexagonal lattice to form a cylinder, see Fig. 1. The sheet can be rolled up in different ways, such that, nanotubes with similar diameters have different chirality. Despite of the fact that the atomic structure of SWNTs is simple, their properties depend dramatically on chirality.¹⁵ SWNTs can be described with a chiral vector C_h given by the unit vectors of the hexagonal lattice a_1 and a_2 , as $C_h = na_1 + ma_2$; where n and m are integers. SWNTs are frequently denoted using these integer number as the nanotube $(n;m)$. The diameter of the nanotube is $d = s/\pi$ where s is the circumferential length of the nanotube, $s = |C_h| = a \sqrt{n^2 + m^2 + nm}$, with a the lattice constant. We can define also the chiral angle ϕ_c as the tilt angle of the hexagons with respect to the direction of the SWNTs axis:

$$\cos \phi_c = \frac{C_h \cdot a_1}{|C_h| |a_1|} = \frac{2n + m}{2 \sqrt{n^2 + m^2 + nm}} : \quad (1)$$

There are only two classes of achiral SW NTs: the arm chair with $n = m$ and $c = 30$, and the zigzag nanotube with $n \neq m$, $m = 0$ and $c = 0$. SW NTs with $0 < c < 30$ are all chiral.

Recently, it has been shown that linear and circular dichroisms can be useful techniques to study SW NTs.^{16,17,18} Quantum mechanical calculations of the influence of chirality on the optical properties of small SW NTs^{17,18,19,20} had been performed. Tasaki et al.,¹⁷ calculated the optical properties of SW NTs using a tight-binding approach. They found that chiral nanotubes are optically active, the CD spectra oscillates, and CD decreases as the diameter increases. However, they did not find a relation between the chiral angle and the strength of CD. Recently, Samsonidze and collaborators¹⁸ also employed a tight binding approach to calculate the electron transitions for chiral SW NTs and circularly polarized light propagating along the nanotube axis. They found the selection rules of the electron transition depending on the handedness of SW NTs that gives rise to optical activity when the time-reversal symmetry is broken, yielding to CD. They calculated the optical absorption for the (20,10) SW NT for left- and right-circularly polarized light. From these spectra, we can infer that they did not find an oscillatory behavior of CD, as Tasaki et al.,¹⁷ did. In both calculations, the tight-binding approximation only accounts for π -band electrons, and other important interactions and effects, like many-body and local field, are not included. In particular, it was found from ab initio calculations that many-body¹⁹ and local field²⁰ effects play important roles to determine the optical properties of nanotubes. Furthermore, local field effect has been pointed out as the main source of the induced optical anisotropy at surfaces of cubic crystals.^{21,22,23} However, quantum mechanical approaches are still inappropriate for systems with hundreds and thousands of atoms due to the huge computational effort that is involved in these type of calculations.

Our goal in this work is to obtain a way to quantify chirality for SW NTs by finding a relation between the chiral angle of SW NTs and their circular dichroism spectra. To explore the capability of the circular dichroism (CD) tool to detect different angles of chirality existing in nanotubes it would be useful to have a theoretical estimation of their CD behavior. We employ a classical electromagnetic model to simulate CD spectra of chiral carbon nanotubes, which includes in an approximated way many body and local field effects. We consider the nanotubes as systems of coupled point dipoles, where the atomic polarizability are obtained from the dielectric function of graphite. The classical approach employs an ansatz in which

a localized polarizable unit in the system in the presence of an external field responds to the local field due to all other induced dipole moments at the other sites plus the external field. This method can treat systems of thousands of atoms for a relatively low cost. It is expected that this information would be useful to motivate further experimental studies to correlate distinctive features of the CD spectra with the different angles of chirality and diameters of SWNTs.

II. DIPOLE APPROXIMATION

To study the optical response of medium size nanotubes we employ the dipole approximation. This approximation has been recently used to study the optical response of chiral gold nanoclusters²⁴, as well as the electron energy loss spectra of SWNTs^{25,26} and fullerenes.²⁷

Let us assume that the SWNTs of interest are composed by N carbon atoms represented by a polarizable point dipole located at the position of the atom. We assume that the dipole located at \mathbf{r}_i , with $i = 1; 2; \dots; N$, is characterized by a polarizability $\alpha_i(\omega)$, where ω denotes the angular frequency. The SWNT is excited by an incident circular polarized wave with wave-vector parallel to the axis of the nanotube. Each dipole of the system is subjected to a total electric field which can be divided into two contributions: (i) $E_{i,inc}$, the incident radiation field, plus (ii) $E_{i,dip}$, the radiation field resulting from all of the other induced dipoles. The sum of both fields is the so called local field given by

$$E_{i,loc} = E_{i,inc} + E_{i,dip} = E_{i,inc} + \sum_{j \neq i} T_{ij} \mathbf{p}_j; \quad (2)$$

where \mathbf{p}_i is the dipole moment of the atom located at \mathbf{r}_i , and T_{ij} is an off-diagonal matrix which couples the interaction between dipoles.^{28,29} On the other hand, the induced dipole moment at each atom is given by $\mathbf{p}_i = \alpha_i E_{i,loc}$, such that $3N$ -coupled complex linear equations are obtained from Eq. (2). These equations can be rewritten as

$$\sum_j (\alpha_i^{-1} \delta_{ij} + T_{ij}) \mathbf{p}_j = \mathbf{M}_{ij} \mathbf{p}_j = E_{i,inc}; \quad (3)$$

where the matrix \mathbf{M} is composed by a diagonal part given by $(\alpha_i^{-1} \delta_{ij})$ and by an off-diagonal

part given by the interaction matrix

$$T_{ij} = \left(\frac{e^{ikr_{ij}}}{r_{ij}^3} k^2 r_{ij} (r_{ij} \cdot p_j) + \frac{(1 - ikr_{ij})}{r_{ij}^2} r_{ij}^2 p_j - 3r_{ij} (r_{ij} \cdot p_j) \right) \quad (4)$$

Here $r_{ij} = r_i - r_j$, $r_{ij} = |r_{ij}|$ and k is the magnitude of the wave vector of the incident electromagnetic field.

The diagonal part in Eqs. (3) is related to the polarizability of each atom, i. e. to the material properties of the system, while the off-diagonal part depends only on the atomic positions, i. e. to the geometrical properties. Once we solve the complex-linear equations shown in Eq. (3), the dipole moment on each atom in the nanotube can be determined, and then we can calculate the extinction cross section, C_{ext} of the SW NT. In terms of the dipole moments,^{28,29}

$$C_{\text{ext}} = \frac{4}{E_0^2} k \sum_{i=1}^N \text{Im} (E_{i,\text{inc}} \cdot p_i) \quad (5)$$

where (\cdot) means complex conjugate.

Circular dichroism is defined as the differential absorption of left (L) and right (R) hand circularly polarized light, which is obtained by subtracting the corresponding extinction efficiencies, Q_{ext} , as

$$CD = Q_{\text{ext}}^R - Q_{\text{ext}}^L \quad (6)$$

Here, the extinction efficiency is defined as $Q_{\text{ext}} = C_{\text{ext}}/A$, where $A = \pi L$, and L is the length of the unit cell of the nanotube. Edge effects due to the finite length of the nanotube are removed by using periodic boundary conditions.

Because chirality is a geometrical property, the CD spectrum will be more sensitive to the second term inside the bracket in Eq. (3), which depends on the atomic geometry, than to the first one that is related to the atomic polarizability. Therefore, the simulated CD spectra will include the geometrical information about the chiral SW NTs. Moreover, it will be crucial for the calculations to have "realistic" atomic positions to obtain the right curvature for each one of the SW NTs studied here.

In this work, we assume that the polarizability for each atom α_i is isotropic and is the same for all the atoms in the nanotube ($\alpha_i = \alpha$). We obtained the polarizability

from the Clausius-Mossotti relation, where the dielectric function of the system was taken from the experimental data for graphite.³⁰ This approximation has been used before to study carbon nanotubes providing good qualitative agreement between calculated optical properties and experimental data.^{25,26,27}

III. ATOMIC STRUCTURES

We obtained the atomic structures of the SW NTs within the density functional theory (DFT) using the siesta computer code.³¹ This code has been widely employed to study the atomic relaxation and electronic properties of small SW NTs.^{32,33,34,35} We used Perdew-Burke-Ernzerhof exchange correlation functional³⁶ within the generalized gradient approximation (GGA). To take into account the interaction between valence electrons and ionic cores, we employed fully non-local norm-conserving pseudopotentials proposed by Troullier and Martins.³⁷ A double polarized (DZP) basis set was used with cutoff radii of 5.12 and 6.25 atomic units for the 2s and 2p orbitals, respectively. In this work, we consider that SW NTs are infinitely long by repeating the unit cell of length L along the nanotube axis. More details of the calculation can be found elsewhere.^{32,33,34,35}

In Table I, we summarized the geometrical parameters obtained in this work using siesta, as labeled in Fig. 1. For comparison, we also include the corresponding parameters of the non-relaxed SW NTs. After relaxation, we found that the chiral vector and diameter of the nanotubes increase by less than 2% with respect to their corresponding non-relaxed (n. r.) values. The bond length in the radial direction, denoted by a in Fig. 1, changes more than the bond lengths in the directions parallel to the axis of SW NTs. These bonds are denoted by b and c in Fig. 1. For SW NTs with diameters about 1 nm, the bond lengths a and c are similar, and they are always larger than b . For SW NTs with larger diameters, the bond lengths a , b , and c become almost equal. The unit cell length, L , is also deviated from its non-relaxed value, increasing approximately 1% in all cases. Then, the bond angles (see Fig. 1) are also modified upon relaxation, such that the α angle is larger, while the β and γ angles tend to be reduced. Our results of the atomic geometry of SW NTs are in excellent agreement with previous DFT calculations for SW NTs with small diameters^{32,33,34,35}.

IV . C I R C U L A R D I C H R O I S M S P E C T R A

We present results for the extinction efficiency and circular dichroism spectrum of different SW NTs. The spectra were calculated using the dipole approximation introduced in Section II, and the atomic positions of SW NTs obtained in Section III. We first present results for the extinction efficiency of SW NTs as a function of the frequency. Then, we discuss the CD spectra for different SW NTs with the same diameter but different chirality, and finally the CD spectra for SW NTs with the same chirality but different diameter.

In Fig. 2 we show the extinction efficiency Q_{ext} in arbitrary units (a. u.) of the SW NT (13,1), as a function of the photon energy of the incident light from 2 eV (620 nm) to 8 eV (155 nm). We observe that Q_{ext} has a maximum at 6.2 eV where absorption effects are dominant, while the asymmetry of the peak is due to scattering effects because the SW NTs considered here are infinitely long. Therefore, a chiral SW NT will show dichroism around these energies. We only show the Q_{ext} for one SW NT, however the same behavior is observed for the rest of the nanotubes.

In Fig. 3 we present the CD spectra for single-wall SW NTs of about the same diameter, $d = 1$ nm, but different chiral angle θ_c . We show the CD in arbitrary units (a. u.) as a function of the photon energy of the incident light from 2 eV to 8 eV. All the spectra show a minimum at 5.2 eV (238 nm) and a maximum at 6.1 eV (203 nm), where light absorption of graphite is more intense.³⁰ From Fig. 3(a), we observe that the CD spectrum is more intense as the chiral angle increases, while in Fig. 3(b) the contrary is observed. For achiral nanotubes, armchair ($\theta_c = 30^\circ$) and zigzag ($\theta_c = 0^\circ$), the CD spectrum is always null. We found that the maximum of the CD spectra is reached when the helicity of the nanotubes is also a maximum, i. e., when θ_c is close to 15° , as shown in the nanotube structures in Fig. 4. For all diameters of SW NTs, we found the same behavior of the CD spectrum as a function of the chiral angle. In summary, we found that the intensity of the CD spectrum depends on the chiral angle of the SW NTs. Therefore, we can conclude that CD measurements can be useful to quantify chirality in these nanostructures.

Now, we analyze the CD spectra for nanotubes of different diameter but same chiral angle. In Fig. 5 we show the CD spectra for nanotubes with (a) $\theta_c = 10:9$ and diameters $d = 1:1; 1:8; \text{ and } 3:3$ nm; with (b) $\theta_c = 16:1$ and diameters $d = 1:0; 2:0; \text{ and } 3:0$ nm, and with (c) $\theta_c = 19:1$ and diameters $d = 1:1; 2:1; \text{ and } 3:1$ nm. For the three cases, we found

that the intensity of the CD spectrum is always larger for smaller diameters. We observe that the maximum of the CD spectra is about half (one third) when the diameter is twice (three times) larger. This is due to the fact that wider nanotubes with the same helicity have a larger surface, such that the chiral effect is less intense. In the limit case, when the diameter goes to infinity, and we recover the hexagonal sheet, the CD will be zero even when ϕ_c will remain unchanged. In summary, we found that there is a relation between the intensity of the CD spectra with the diameter of the nanotube. From these results, we can conclude that CD measurements can be also useful to quantify the diameter of chiral SWNTs.

V. CONCLUSIONS

Using the computer code called *siesta*, within the density functional theory, we obtained the atomic positions of 14 different single-wall carbon nanotubes such that most of them were not reported before in the literature. Our DFT results are in excellent agreement with previous calculations of smaller single-wall carbon nanotubes. Furthermore, we have studied the circular dichroism optical spectra of these single-wall carbon nanotubes of different diameters and chirality within a dipole approximation. We found that for nanotubes with a given diameter, the intensity of circular dichroism spectra increases as the helicity of the nanotube also does. We also found that the intensity of the circular dichroism spectra of single-wall nanotubes, for a given chiral angle, depends on the diameter of the nanotube, such that wider nanotubes show a less intense spectra. From these results, we can conclude that circular dichroism measurements can be useful to quantify chirality as well the diameters of chiral SWNTs. It is expected that this information would be useful to motivate further experimental studies in this direction.

Acknowledgments

We acknowledge the fruitful discussion with Ignacio L. Garzon. Partial financial support from DGAPA-UNAM grant No. IN101605, and VIEP-BUAP II193-04/EXC/G is also

acknowledged.

Corresponding author. Email: cecilia@sisca.unam.mx

- ¹ L. D. Barron, *Nature* 405, 895 (2000).
- ² G. L. J. A. Rikken and E. Raupach, *Nature* 405, 932 (2000).
- ³ B. B. Smimov, O. V. Lebedev, A. V. Evtushenko, *Acta Cryst. A* 55, 790 (1999).
- ⁴ A. B. Buda, K. M. Islow, *J. Am. Chem. Soc.* 114, 6006 (1992).
- ⁵ Bellarosa, L.; Zerbetto, F. *J. Am. Chem. Soc.* 125, 1975 (2003).
- ⁶ W. J. Richter, B. Richter, E. Ruch, *Angew. Chem.* 85, 20 (1973).
- ⁷ T. Damhus, C. E. Schaer, *Inorg. Chem.*, 22, 2406 (1983).
- ⁸ L. A. Kutulya, V. E. Kuz'min, I. B. Stelmakh, T. V. Handrinailova, P. P. Shtifanyuk, *J. Phys. Org. Chem.* 5, 308 (1992).
- ⁹ H. Zabrodsky, S. Peleg, D. Avnir, *J. Am. Chem. Soc.* 114, 7843 (1992); *ibid.* 115, 8278 (1993); *ibid.* 117, 462 (1995).
- ¹⁰ G. Moreau, *J. Chem. Inf. Comput. Sci.* 37, 929 (1997).
- ¹¹ J. Maruani, G. Gilat, R. Veyssere, C. R. Acad. Sci. Ser. 2. Fasc, 319, 1165 (1994).
- ¹² P. E. auf der Heide Thomas, A. B. Buda, K. M. Islow, *J. Math. Chem.* 6, 255 (1990).
- ¹³ M. Nogradi, *Stereoselective Synthesis: A Practical Approach*, Wiley-VCH, Weinheim { New York (1995).
- ¹⁴ V. I. Sokolov, N. F. Standen (Translator), *Introduction to Theoretical Stereochemistry*, Gordon & Breach Science Pub, Amsterdam (1991).
- ¹⁵ R. Saito, G. Dresselhaus, M. S. Dresselhaus, *Physical Properties of Carbon Nanotubes*; Imperial College Press: London, U.K., 1998.
- ¹⁶ J. Rajendra, M. Baxendale, L. G. DittRap, A. Rodger, *J. Am. Chem. Soc.* 126, 11182 (2004).
- ¹⁷ S. Tasaki, K. Maekawa, T. Yamabe, *Phys. Rev. B* 57, 9301 (1998).
- ¹⁸ G. G. Samsonidze, A. Gunelis, R. Saito, A. Jorio, A. G. Souza Filho, G. Dresselhaus, and M. S. Dresselhaus, *Phys. Rev. B* 69, 205402 (2004).
- ¹⁹ E. Chang, G. Bussi, A. Ruini, and E. Molinari, *Phys. Rev. Lett.* 92, 196401 (2004).
- ²⁰ A. G. Marinopoulos, L. Reining, A. Rubio, and N. Vast, *Phys. Rev. Lett.* 91, 046402 (2003).
- ²¹ W. L. Mochan, R. G. Barrera, *Phys. Rev. Lett.* 55, 1192 (1985).

- ²² B. S. Mendoza, W. L. Mochar, Phys. Rev. B 53, R10473 (1996).
- ²³ C. D. Hogan, C. H. Patterson, Phys. Rev. B 57, 14843 (1998).
- ²⁴ C. E. Román-Velázquez, C. Noguez, I. L. Garzon, J. of Phys. Chem. B 107 12035 (2003).
- ²⁵ A. Rivacoba, F. J. García de Abajo, Phys. Rev. B 67, 085414 (2003).
- ²⁶ X. H. Wu, L. S. Pan, H. Li, X. J. Fan, T. Y. Ng, D. Xu, C. X. Zhang, Phys. Rev. B 68, 193401 (2003).
- ²⁷ L. Henrard, Ph. Lambin, J. Phys. B: At. Mol. Opt. Phys. 29, 5127 (1996).
- ²⁸ E. M. Purcell, C. R. Pennypacker, Astrophys. J. 186, 705 (1973).
- ²⁹ B. T. Draine, Astrophys. J. 333, 848 (1998).
- ³⁰ D. L. Greenaway, G. Harbeke, F. Bassani, E. Tosatti, Phys. Rev. 178, 1340 (1969).
- ³¹ S. Sanchez-Portal, P. Ordejón, E. Artacho, J. M. Soler, Int. J. Quantum Chem. 65, 453 (1997).
- ³² M. Machon, S. Reich, C. Thomsen, D. Sanchez-Portal, P. Ordejón, Phys. Rev. B 66, 155410 (2002).
- ³³ S. Reich, C. Thomsen, P. Ordejón, Phys. Rev. B 65, 153407 (2002).
- ³⁴ S. Reich, C. Thomsen, P. Ordejón, Phys. Rev. B 65, 155411 (2002).
- ³⁵ S. Reich, C. Thomsen, P. Ordejón, Phys. Rev. B 64, 195416 (2001).
- ³⁶ J. P. Perdew, K. Burke, M. Ernzerhof, Phys. Rev. Lett. 77, 3685 (1996).
- ³⁷ N. Troullier, J. L. Martins, Phys. Rev. B 43, 1993 (1991).

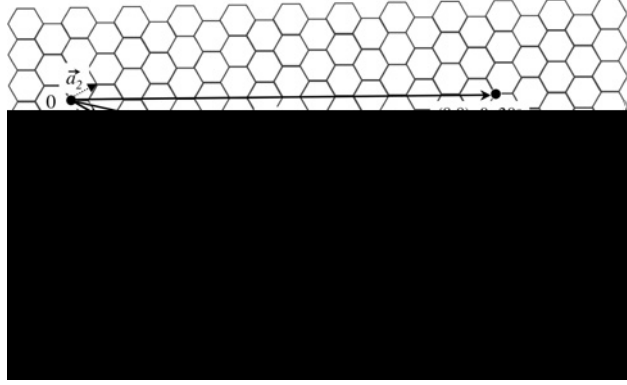


FIG .1: Model of the atomic geometry of a hexagonal two-dimensional lattice with unit vectors \mathbf{a}_1 and \mathbf{a}_2 .

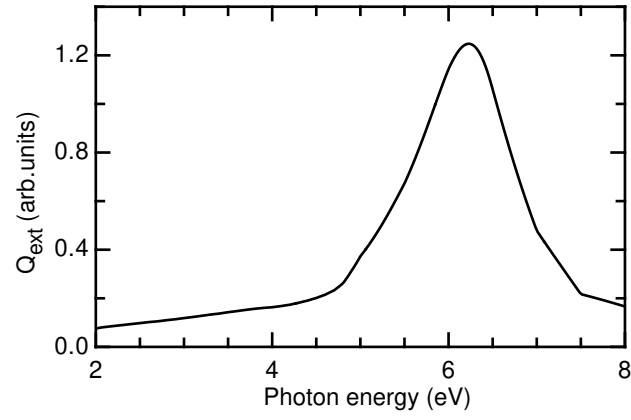


FIG .2: Extinction efficiency of the SW NT (13,1).

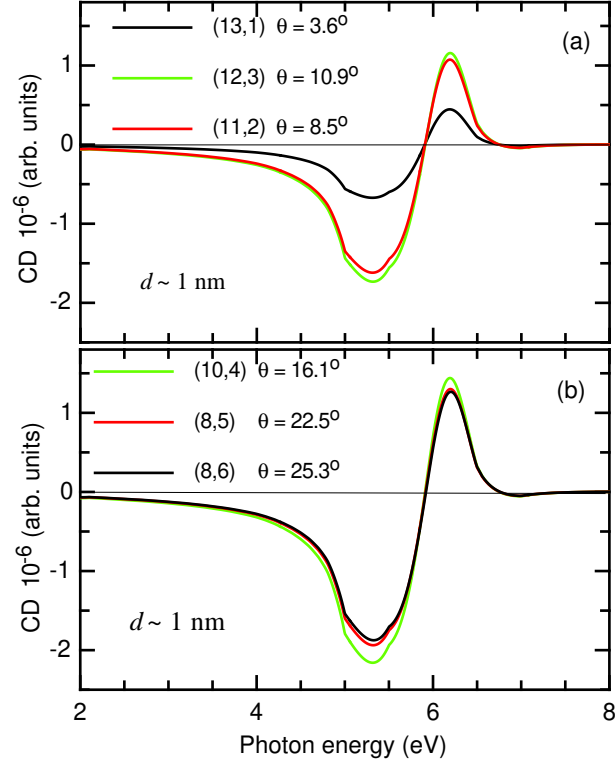


FIG .3: (Color online) CD spectra of SW NTs with the same diameter $d = 1$ nm and (a) $0^\circ \leq \theta \leq 15^\circ$, and (b) $15^\circ \leq \theta \leq 30^\circ$.

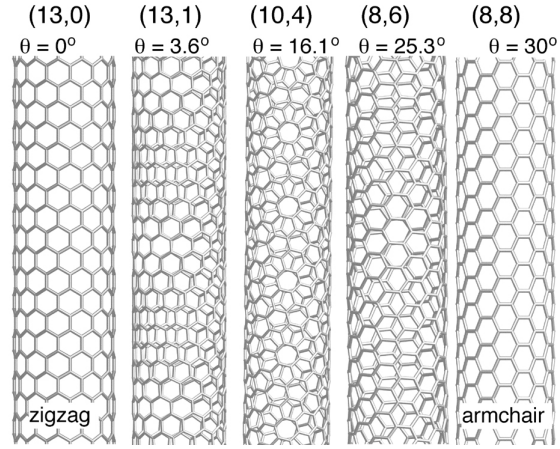


FIG .4: Structure of single-wall SW NTs with different chiral angles between 0° and 30° .

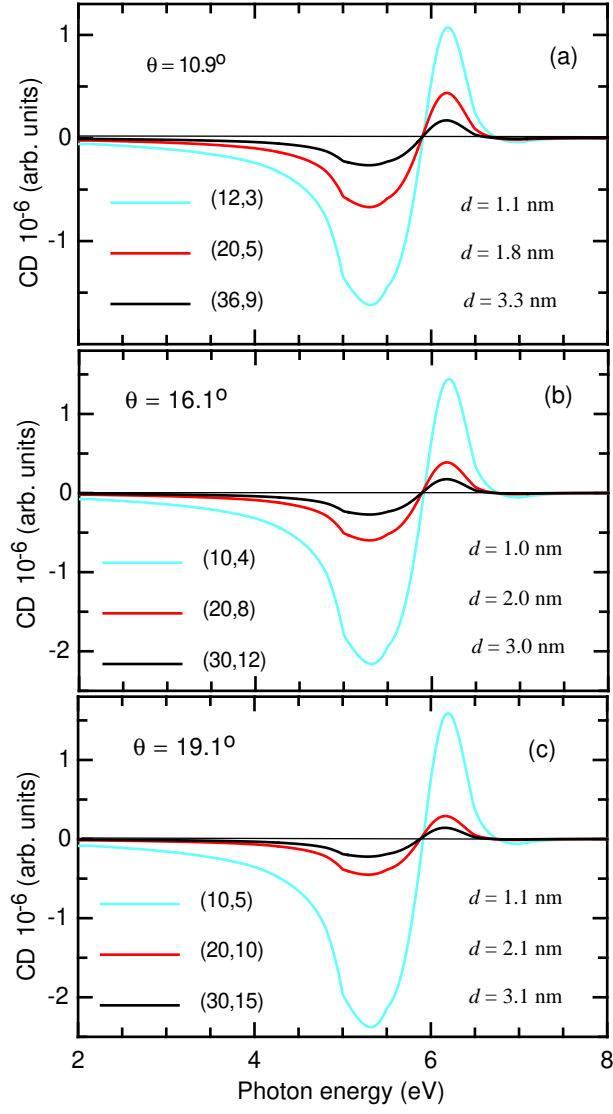


FIG . 5: (Color online) CD spectra of SW NTs of different diameter but same chiral angle (a) $\theta_c = 10.9^\circ$, (b) $\theta_c = 16.1^\circ$, and (c) $\theta_c = 19.1^\circ$.

(n,m)	α_c	β_{hj} ($^\circ$)	a(\AA)	b(\AA)	c(\AA)			
(13,1)	3.6	34.46	1.46	1.45	1.46	118.8	120.0	119.9
n. r.		33.74	1.44	1.44	1.44	118.6	120.1	120.0
(26,2)	3.6	10.87	1.45	1.45	1.46	119.7	120.0	120.0
n. r.		10.74	1.44	1.44	1.44	119.6	120.0	120.0
(11,2)	8.5	30.76	1.46	1.45	1.46	118.5	120.0	119.8
n. r.		30.24	1.44	1.44	1.44	118.3	119.9	120.1
(12,3)	10.9	34.80	1.46	1.46	1.46	118.9	119.9	119.8
n. r.		34.29	1.44	1.44	1.44	118.7	120.1	119.9
(20,5)	10.9	57.84	1.46	1.45	1.46	119.6	120.0	119.9
n. r.		57.11	1.44	1.44	1.44	119.5	120.0	119.5
(36,9)	10.9	103.95	1.45	1.45	1.46	119.9	120.0	120.0
n. r.		102.87	1.44	1.44	1.44	119.8	120.0	120.0
(10,4)	16.1	31.67	1.46	1.45	1.46	118.8	119.8	119.7
n. r.		31.15	1.44	1.43	1.44	118.6	120.1	119.7
(20,8)	16.1	63.05	1.46	1.45	1.46	119.7	120.0	119.9
n. r.		62.30	1.44	1.44	1.44	119.7	120.0	119.9
(30,12)	16.1	63.99	1.47	1.47	1.47	119.9	120.0	120.0
n. r.		56.50	1.44	1.44	1.44	119.8	120.0	120.0
(10,5)	19.1	33.52	1.46	1.45	1.46	119.0	119.8	119.7
n. r.		32.99	1.44	1.43	1.44	118.9	120.1	119.7
(20,10)	19.1	66.76	1.46	1.46	1.46	119.8	120.0	119.9
n. r.		65.97	1.44	1.44	1.44	119.7	120.0	119.9
(30,15)	19.1	100.03	1.45	1.45	1.46	119.9	120.0	120.0
n. r.		98.96	1.44	1.44	1.44	119.9	120.0	120.0
(8,5)	22.4	28.84	1.46	1.45	1.46	118.9	119.6	119.5
n. r.		28.33	1.44	1.43	1.44	118.6	119.4	120.0
(8,6)	25.3	30.85	1.46	1.45	1.46	119.1	119.6	119.6
n. r.		30.34	1.44	1.43	1.44	118.9	119.4	120.0

TABLE I: Geometrical parameters as defined in Fig. 1 for relaxed and non-relaxed (n. r.) SWNTs.

α_c , β_{hj} , and β_{ij} are given in degrees.